Canadian Journal of Applied Sciences; 2011; 1(2): 50-67, July, 2011
Intellectual Consortium of Drug Discovery & Technology Development Inc.
ISSN 1925-7430 Available online http://www.canajas.com

Original Research Article

EFFECTS OF SLIP ON FLOW BETWEEN TWO STRETCHABLE DISKS USING OPTIMAL HOMOTOPY ANALYSIS METHOD

Sufian Munawar[1,*], Ahmer Mehmood[2], Asif Ali[1]

[1]Department of Mathematics Quaid-i-Azam University Islamabad Pakistan.

[2]Department of Mathematics (FBAS) International Islamic University Islamabad Pakistan

ABSTRACT

This work presents the analytic solution of flow of a viscous fluid between two stretching disks with slip boundaries. Suitable similarity transformations are used to normalize the governing system. Optimal homotopy analysis method has been used as a solution technique by considering one parameter; two parameters; three parameters and one step optimal HAM approaches. The solutions obtained through all these approaches are compared. It is observed that, although the solution series (obtained through Optimal HAM) attains convergence at initial few terms but, on the other hand the computational resources,required to acquire solution, increases indefinitely as we increase the order of approximation.The current analytic solution is compared with a numerical technique and it is found that both solutions are perfectly matched. The effects of material parameters on different physical quantities are illustrated through graphs and tables.

Key words: Stretching disks, slip conditions, analytic solution, optimal HAM

***Corresponding Author**: [1]Department of Mathematics Quaid-i-Azam University Islamabad Pakistan. Email: sufian.munawar@hotmail.com, Tel. +92-333-5756965

1. INTRODUCTION

The boundary layer flow due to moving or stretching surfaces has been investigated broadly in the field of fluid mechanics. Such kinds of studies are very essential, practically, in engineering and industrial processes. In the manufacturing of metallic and polymeric solid cylinders and sheets it is observed experimentally by Vleggaar [1], that the velocity of the material is approximately proportional to the distance, so such kinds of system are mathematically modeled as stretching sheets, disks and cylinders. Theoretically, the pioneer work on viscous flow due tomoving surfacewas initiated by Sakiadis [2]. Exact solutions for the flows due to stretching

surface were obtained by Crane [3] and Wang [4]. Motivated by the ideas of afore mentioned authors various researchers explored the flow over stretching surfaces in different circumstances.Andersson [5] investigated the boundary layer flow of an electrically conducting non-Newtonian fluid past a stretching sheet. Troy [6] investigated the issue of uniqueness for a second grade fluid over a stretching sheet.Carragher and Crane [7] studied the heat transfer phenomena on a continuous stretching sheet.Grubka and Bobba [8] performed heat transfer analysis by considering the variable temperature property. Kumari et al. [9] studied heat transfer characteristic in MHD flow over a stretching sheet with prescribed wall temperature or heat flux.Elbashbeshy [10] extended the study of heat transfer over a stretching sheet to the case with variable surface heat flux. Ali and Mehmood [11] discussed the unsteady flow over stretching sheet in porous medium with suction and injection on the surface. Mehmood and Ali [12] investigated the analytic series solution for the generalized three-dimensional flow and heat transfer over a stretching sheet which is valid for whole range of stretching parameter. The study was then further extended to the case where the stretching surface is not essentially flat. The flow over a stretching cylinder was first instigated by Wang [13] who studied the flow due to the uniform stretching of cylinder surrounded by fluid at rest.The axisymmetric flow of a viscoelastic fluid over a radially stretching disk was studied by Ariel [14] in which the perturbation solution for small Deborah number and asymptotic solution for large Deborah number were obtained.Three-dimensional flow over a radially stretching and coaxially rotating disk was investigated by Fang [15] by taking into account the cases of only stretching disk and both rotating and stretching disk. Zaturska and Banks [16] discussed the flow between a channel with porous and stretching boundaries. Currently, Fang and Zhang [17] modified the problem of Ariel [14] by taking a viscous fluid between two coaxial infinite radially stretching disks with different stretching rates and solved the equations using the shooting method. Gorder et al. [18] confirmed the results of Fang and Zhang [17] via a strongly analytic technique homotopy analysis method and showed a good agreement.

The objective of present study is to investigate the effects of slip condition on the similarity flow between two stretching disks and to report the advantages and limitations of some new analytical solution technique, namely, optimal HAM proposed by Liao [19] and one step optimal HAM given by Niu and Wang [37]. The basic idea of homotopy analysis method (HAM) was outset by Liao [20] to get the analytic series solution of nonlinear differential equations in his doctoral thesis in 1994. But it was later observed that the solution series obtained from this early version of HAM often does not converge. In 1999 Liao [21] established a novel form of the zeroth order deformation equation of HAM by introducing a non-zero auxiliary parameter $\hbar$as:

$$(1-p)\mathcal{L}[F(x;p)-f_0(x)] = \hbar p\mathcal{N}[F(x;p)], \quad (1)$$

where $p \in [0,1]$ the embedding parameter related to the mapping $F(x;p)$ which deforms continuously from $f_0(x)$ to $f(x)$ as p varies form 0 to 1, $\mathcal{N}$ is a nonlinear operator and $f_0(x)$ is the initial guess for the exact solution $f(x)$. $F(x;p)$can be expanded in the form of a Taylor series

$$F(\eta;p) = f_0(\eta) + \sum_{m=1}^{\infty} f_m(\eta)p^m, \quad (2)$$

whichif converges to the exact solution at $p = 1$, we get the HAM series solution

$$f(\eta) = f_0(\eta) + \sum_{m=1}^{\infty} f_m(\eta). \quad (3)$$

The convergence of above solution series strongly depends upon the auxiliary parameter $\hbar$. This parameter $\hbar$ controls the rate and region of convergence of homotopy series solution (3)and therefore named as convergence-control parameter [22]. This traditional homotopy analysis method is successfully applied by many authors [23-34] to solve highly nonlinear ordinary and partial differential equations.Recently, more generalized form of zeroth order deformation equation (1) is given by Liao [34] as

$$(1 - B(p))\mathcal{L}[F(x;p) - f_0(x)] = \hbar A(p)\mathcal{N}[F(x;p)], \quad (4)$$

where$A(p)$ and $B(p)$ are deformation functions satisfying the properties

$$A(0) = B(0) = 0 \text{and } A(1) = B(1) = 1. \quad (5)$$

As there are infinite numbers of ways of choosing these deformation functions so we have more freedom of choice to ensure the convergence of series by choosing appropriate form of deformation functions. This freedom of choice is further utilized by Marinca et al. [35] in his so called optimal homotopy asymptotic method (OHAM). Marinca pooled $\hbar$ and $A(p)$ as a one function,$H(p)$ with the property that $H(0) = 0$ and $H(1) \neq 1$ and formulated the deformation equation of the form

$$(1 - p)\mathcal{L}[F(x;p) - f_0(x)] = H(p)\mathcal{N}[F(x;p)], \quad (6)$$

where$H(p)$ is expanded by the Taylor series $\sum_{n=1}^{\infty} \hbar_n p^n$.

The issue of selection of suitable value of convergence control parameter $\hbar$ has been resolved byYabushitaet al. [36] who proposed an optimization method for two coupled ordinary differential equations, based on the integration of residual error ε_N given by

$$\varepsilon_N = \left[\left(\int_\Omega \mathcal{N}_1[f_N, g_N]\, d\Omega\right)^2 + \left(\int_\Omega \mathcal{N}_2[f_N, g_N]\, d\Omega\right)^2\right]^{1/2}, \quad (7)$$

wheref_N and g_N are solution at the $N$the order of approximation. It was determined by Yabushita et al. [36] that the approximate series solution by HAM approaches to the exact solution if ε_N tends to zero. The optimized value of convergence controlling parameters can be obtained by minimizing the residual error $\log_{10} \varepsilon_N$by plotting the contour against convergence controlling parameters. Marinca [35] obtained the optimized values of convergence controlling parameters using the square residual error $\Delta_N(\hbar_1, \hbar_2, \ldots, \hbar_N)$ given by

$$\Delta_N(\hbar_1, \hbar_2, \ldots, \hbar_N) = \int_\Omega (\mathcal{N}[\sum_{m=1}^{\infty} f_m(\eta)])^2 d\Omega, \quad (8)$$

and minimized the square residual error utilizing the fist derivative law of Calculus as

$$\frac{\partial \Delta_N(\hbar_1, \hbar_2, \ldots, \hbar_N)}{\partial \hbar_k} = 0, \ (1 \leq k \leq N), \quad (9)$$

which corresponds to Nnonlinear algebraic equations with Nunknowns but in this approach,as the order of approximation increases by one, the number of eqs.(9) alsogrow by one with one additional unknown and for large N the system of algebraic eqs. (9) becomesa great dealand more computations are required to calculate the unknowns form eqs. (9). More recently, Niu and Wang et al. [37] reported that it is practically more tedious to calculate the optimal values of $\hbar_k$ from the highly nonlinear and sparse system of algebraic equations. To overcome the drawbacks of Marinca approach Niu and Wang [37] suggested the one-step optimal homotopy analysis method. According to this approach the CPU time and memory losses can be reduced if the

residual error isminimized at each order of approximation. In this way, we can obtain the value of each $\hbar_N$ at Nth-order by solving only one nonlinear algebraic equation with one unknown. Obviously, in this approach less computational resources are required than that of the Marinca's approach. Unfortunately, this one-step optimal HAM is valid only for small values of parameters as pointed out by Niu and Wang [37] in the same paper and this downside of the method is also observed in the present work.

Currently, Liao introduced a new three-parameter optimal homotopyanalysis method in a recent paper [19]. Optimal HAM is based on the generalized zeroth order deformation eq. (4) with the unique type of deformation functions each depending upon the characteristic parameters $|c_1| \ll 1$ and $|c_2| \ll 1$. Liao also suggested a new sort of approximation to exact square residual error to accelerate the efficiency of computation. Liao applied this approach effectively to the well-knownand simplest Blasius flow problem and obtained the solution which converges at the earlier order of approximation than that of traditional HAM. However, it is a misfortune that the solution series given by optimal HAMcontains three unknown convergence control parameters. Therefore, it is sometime impractical to obtain the solution at the higher order of approximation with three unknown parameters as the CPU time increases exponentially as shown later in this paper and a hefty random access memory RAM is required to reach at suitable accuracy.In the current study we investigate the merits and limitations of different optimal HAM approaches by providing the convergence, accuracy and efficiency of all approaches based on homotopy. All calculations are performed on a PC Core i7 3.2 GHz CPU with 8 GB RAM using the symbolic computational software Mathematica.

2. FORMULATION OF PROBLEM

Consider a steady state laminar flow of an incompressible viscous fluid between two continuously stretching coaxial disks.Because of the presence of slip condition at the walls of disks, the velocities of linearly stretching lower and upper disks $a_1 r$and $a_2 r$ are balanced by the shear rates$\lambda_1 \frac{\partial u}{\partial z}$and $\lambda_1 \frac{\partial u}{\partial z}$at the walls, respectively.Further we assume that the centers of surfaces are held fixed and the disks are stretching along the radial direction r while z is the axial coordinateperpendicular to radial direction. The lower disk is located at $z = 0$ while the upper disk is at distance d apart.

According to the above assumptions, the equations that govern the considered flow problem are the continuity equation and the Navier-Stokes equations which take the form:

$$\frac{\partial u}{\partial r} + \frac{u}{r} + \frac{\partial w}{\partial z} = 0, \tag{10}$$

$$u\frac{\partial u}{\partial r} + w\frac{\partial u}{\partial z} = -\frac{1}{\rho}\frac{\partial p}{\partial r} + \nu\left[\frac{\partial^2 u}{\partial r^2} + \frac{\partial}{\partial r}\left(\frac{u}{r}\right) + \frac{\partial^2 u}{\partial z^2}\right], \tag{11}$$

$$u\frac{\partial w}{\partial r} + w\frac{\partial w}{\partial z} = -\frac{1}{\rho}\frac{\partial p}{\partial z} + \nu\left[\frac{\partial^2 w}{\partial r^2} + \frac{1}{r}\frac{\partial w}{\partial r} + \frac{\partial^2 w}{\partial z^2}\right]. \tag{12}$$

Subject to the boundary conditions

$$u(r,z) = ra_1 + \lambda_1\frac{\partial u}{\partial z}, \quad w(r,z) = 0, \quad \text{at} \quad z = 0, \tag{13}$$

$$u(r,z) = ra_2 + \lambda_2\frac{\partial u}{\partial z}, \quad w(r,z) = 0, \quad \text{at} \quad z \to d. \tag{14}$$

To normalize the above system of eqs (10)-(14) the Von Kármán type of similarity transformations are used

$$u = ra_1F'(\zeta), \quad w = -2da_1F(\zeta), \quad \zeta = \frac{z}{d}, p = \rho a_1 \nu \left[P(\zeta) + \frac{1}{2}\frac{r^2}{d^2}\beta\right]. \tag{15}$$

Using these transformations in eqs (10)-(14), eq. (10) satisfies identically and we left with the following system of ordinary differential equations:

$$F''' + Re[2FF'' - (F')^2] + \beta = 0, \tag{16}$$

$$P' = 4ReFF' + 2F'', \tag{17}$$

with the boundary conditions

$$F(0) = 0, \qquad F'(0) = 1 + Kn_1F''(0), \qquad P(0) = 0, \tag{18}$$

$$F(1) = 0, \qquad F'(1) = A + Kn_2F''(1), \tag{19}$$

whereprime denotes the differentiation with respect to ζ, $Re = a_1d^2/\nu$ is the Reynolds number proportional to the lower disk stretching rate, A is the ratios of disks stretching velocities and $Kn_1 = \frac{\lambda_1}{L}$ and $Kn_2 = \frac{\lambda_2}{L}$ are the Knudsen numbers.

To acquire more simplified form and to eliminate β, eq. (16) can be differentiated with respect to ζ as follows:

$$F^{iv} + 2ReFF''' = 0, \tag{20}$$

andthe pressure parameterβ can be determined by the boundary conditions (18) as

$$\beta = Re\,[F'(0)]^2 - F'''(0). \tag{21}$$

The pressure term can be calculated by integrating eq. (17) and using the boundary conditions (18) as

$$P = 2[ReF^2 + F' - F'(0)]. \tag{22}$$

The shear stressτ_{zr}at the surface of lower disk in radial and tangential direction is given by

$$\tau_{zr} = \mu\left(\frac{\partial u}{\partial z}\right)_{z=0} = \frac{\mu r a_1}{d}F''(0). \tag{23}$$

Accordingly, the coefficient of skin friction $C_f$at the lower disk reduces to

$$C_f = \frac{\tau_w}{\rho(ra_1)^2} = \frac{1}{Re_r}F''(0), \tag{24}$$

where$Re_r = ra_1d/\nu$ is the local Reynolds number.

3. METHOD OF SOLUTION

To find out the solution of equation (20) subject to the boundary conditions (18) and (19) we use the three parameters optimal homotopy analysis method. According to the nature of boundary conditions we seek the solution series of the form

$$f(\zeta) = \sum_{m=0}^{\infty} a_m \zeta^m, \tag{25}$$

where a_m are the coefficients of the series. Conferring the boundary conditions we choose the initial guess

$$f_0(\zeta) = \frac{(2Kn_1A+4Kn_2-1)\zeta-(6Kn_2-A-2)\zeta^2-(2Kn_1A-2Kn_2+A+1)\zeta^3}{12Kn_1Kn_2-4Kn_1+4Kn_2-1}, \quad (26)$$

and linear operator of the form

$$\mathcal{L} \equiv \frac{\partial^4}{\partial\zeta^4}. \quad (27)$$

Using the governing eq. (20) we define the non-linear operator $\mathcal{N}\left[\hat{F}(\zeta;p))\right]$as

$$\mathcal{N}\left[\hat{F}(\zeta;p))\right] = \frac{\partial^4\hat{F}(\zeta,p)}{\partial\zeta^4} + 2Re\,\frac{\partial\hat{F}(\zeta,p)}{\partial\zeta}\frac{\partial^3\hat{F}(\zeta,p)}{\partial\zeta^3}. \quad (28)$$

According to the threeparameter optimal homotopy analysis method [19] the so called zeroth order deformation equation can be written as

$$\left(1-B(p;c_2)\right)\mathcal{L}\left[\hat{F}(\zeta;p)-\hat{F}_0(\zeta)\right] = c_0A(p;c_1)\mathcal{N}\left[\hat{F}(\zeta;p))\right], \quad (29)$$

subject to the boundary conditions

$$\hat{F}(\zeta;p) = 0, \quad \frac{\partial\hat{F}(\zeta,p)}{\partial\zeta} = 1 + Kn_1\frac{\partial^2\hat{F}(\zeta,p)}{\partial\zeta^2}, \text{ at}\zeta = 0, \quad (30)$$

$$\hat{F}(\zeta;p) = 0, \quad \frac{\partial\hat{F}(\zeta,p)}{\partial\zeta} = A + Kn_2\frac{\partial^2\hat{F}(\zeta,p)}{\partial\zeta^2}, \text{ at}\zeta = 1, \quad (31)$$

where$0 \neq c_0$, c_1 and c_2 are convergence control parameters,$p \in [0,1]$is the embedding parameter related to the mapping$\hat{F}(\zeta;p)$which deforms continuously from $F_0(\zeta)$ to $F(\zeta)$ as p varies form 0 to 1,$A(p;c_1) = \sum_{m=1}^{\infty}\mu_m(c_1)p^m$ and $B(p;c_2) = \sum_{m=1}^{\infty}\sigma_m(c_2)p^m$ are the deformation functions with $\mu_m(c_1) = (1-c_1)c_1^{m-1}$, $\sigma_m(c_2) = (1-c_2)c_2^{m-1}$, $|c_1| < 1$ and $|c_2| < 1$, satisfying the property (5). Expanding $\hat{F}(\zeta;p)$ in Taylor series with respect to $p$we have

$$\hat{F}(\zeta;p) = F_0(\zeta) + \sum_{m=1}^{\infty}F_m(\zeta)p^m, \quad (32)$$

where

$$F_m(\zeta) = \frac{1}{m!}\frac{\partial^m\hat{F}(\zeta;p)}{\partial p^m}\bigg|_{p=0}. \quad (33)$$

The mth-order deformation equation can be obtained by differentiating eqs. (29-(31) m-times with respect to $p$and dividing by $m!$ in the form

$$\mathcal{L}[F_m(\zeta) - \sum_{k=0}^{m-1}\chi_{k+1}\sigma_{m-k}(c_2)F_k(\zeta)] = c_0\sum_{k=0}^{m-1}\mu_{m-k}(c_1)\delta_k(\zeta), \quad (34)$$

subject to the boundary conditions

$$F_m(0) = 0, \quad \frac{\partial F_m(0)}{\partial\zeta} = Kn_1\frac{\partial^2F_m(0)}{\partial\zeta^2}, \text{and } F_m(1) = 0, \frac{\partial F_m(1)}{\partial\zeta} = Kn_2\frac{\partial^2F_m(1)}{\partial\zeta^2} \quad (35)$$

where

$$\delta_k(\eta) = \frac{1}{k!}\frac{\partial^k\mathcal{N}[\hat{F}(\zeta;p)]}{\partial p^k}\bigg|_{p=0} = \frac{\partial^4F_k(\zeta)}{\partial\zeta^4} + 2Re\sum_{j=0}^{k}F_j(\zeta)\frac{\partial^2F_{k-j}(\zeta)}{\partial\zeta^2}, \quad (36)$$

and

$$\chi_k = \begin{cases} 0, & k \leq 1, \\ 1, & k > 1. \end{cases} \quad (37)$$

Let $F_m^*(\zeta)$ represents a particular solution of eq. (34) then the general solution can be written in the form

$$F_m(\zeta) = F_m^*(\zeta) + \sum_{k=0}^{m-1} \chi_{k+1} \sigma_{m-k}(c_2) F_k(\zeta) + A_1 + A_2\zeta + A_3\zeta^2 + A_4\zeta^3, \quad (38)$$

in which $A_i (i = 1,2,3,4)$ are constants of integration and can be determined using the boundary conditions (35). The above system of linear non-homogeneous ordinary differential equations (34) along with the boundary conditions (35) is solved up to the sufficient order of approximation to achieve the complete solution of original differential equations (18)-(20) in the form of an infinite series of functions i.e.

$$F(\zeta) = F_0(\zeta) + \sum_{m=1}^{\infty} F_m(\zeta). \quad (40)$$

Note that at any order of approximation the above solution series (40) contains three unknown convergence controlling parameters c_0, c_1 and c_2 with the help of which we can determine the convergence rate and region of solution series. By choosing the optimal values of these convergence controlling parameters we can achieve the convergence of solution series more rapidly.To obtain the optimal values of c_0, c_1 and c_2 we first calculate the square residual error using the following formula given by Liao [19]:

$$E_m = \sqrt{\frac{1}{N+1} \sum_{j=0}^{N} \left[\mathcal{N}(f_j)\right]^2}, \quad (41)$$

where $f_j = f(j\Delta\zeta)$ is the discretization of continuous function $f(\zeta)$into N pieces by choosing $\Delta\zeta = 0.05$ and $N = 20$for our problem. The best values of c_0, c_1 and c_2 can be found where the square residual error E_m is minimum. The minimum of $E_m$can be calculated using the first derivative law of Calculus. The values of c_0, c_1 and c_2 are calculated by simultaneously solving the three algebraic equations

$$\frac{\partial E_m}{\partial c_0} = 0, \quad \frac{\partial E_m}{\partial c_1} = 0 \text{and} \frac{\partial E_m}{\partial c_2} = 0. \quad (42)$$

4. Convergence and accuracy of method

To investigate the convergence and accuracy of the different homotopy approaches we will give a brief comparison of different approaches in this section. According to Liao [19], the two standards for an adequate method to solve nonlinear equations are that it can approximate the expressions efficiently and accurately for the suitable values of physical parameters. We will analyze the convergence, accuracy and efficiency of different analytic techniques for the considered problem in this section. To accelerate the convergence of our solution we use the homotopy padé approximation on the solution series given by different methods using the best values of convergence control parameters and the results are listed in table 1.

In case of one parameter optimal HAM $(c_1 = c_2 = 0)$, the convergence is controlled by only one parameter c_0 and the deformation equation (29) reduces to the traditional HAMequation(1). Therefore the solution obtained by one parameter optimal HAM corresponds to traditional HAM techniques. At 20th order of approximation the optimized value of c_0 is calculated to be -1.082301. At this optimized value of c_0 the tabulated values of $f''(0)$are given in Table 1

using the homotopy padé approximation. It is observed form the table that after 12th order of approximation there are no corrections up to 6 decimal places. The square residual error E_m is calculated in table 2. It is noted that as the order of approximation increases the corresponding residual error decreases significantly and at 30th order of approximation the residual error reaches to 2.27126×10^{-5}.

In the two parameter optimal HAM approach, there are two convergence control parameters c_0 and c_1 (as $c_1 = c_2$). The optimal values of $c_0 = -1.385313$ and $c_1 = 0.218662$ are obtained by minimizing the square residual error E_{20} at the 20th order. The corresponding homotopy padé approximations for $f''(0)$ using the optimal values of c_0 and c_1 are shown in table 1 and no significant differences are observed between one and two parameters approaches. In fig. 1 the square residual error is plotted against c_1 at the fixed optimized value of c_0 at the 6th, 8th and 12th order of approximation and it is noted that as the order of approximation increases the square residual error moves toward zero by giving the optimal value of c_1. This comparison demonstrates that the two parameters optimal homotopy analysis approach converges at same order as compared with one parameter approach although; sympathetically, more computational time and recourses are required to calculate the solution of two parameters optimal HAM approach as compared to the one parameter approach which is described in table 3.

In the three parameter optimal homotopy analysis method, three parameters are introduced to control the convergence of solution series. By minimizing the square residual error E_{20} at 20th order of approximation, the optimal values of convergence-controlling parameters are obtained as $c_0 = -1.509902$, $c_1 = 0.201629$ and $c_2 = 0.337949$. Form table 1 it is noticed that at these optimized values of convergence control parameters the corresponding padé approximation for $f''(0)$ converges at 6th order. It is interesting to note that the square residual error in the case of three parameters optimal approach moves toward zero drastically as compared to other optimal approaches (see table 2). Therefore it is examinedfrom here that three parameters optimal HAM approach converges at earlier order of approximation than those discussed before. Nevertheless, due to three unknown parameters much more computations are required to calculate the solution at the high order of approximation as shown in table 3 and practically it is sometime unfeasible to calculate the solutionespecially for the system of highly nonlinear differential equations.

From table 1 it is important to note that the solution obtained through one step optimal HAM approach given by Niu and Wang [37] though convergesbut not accurately to the exact value. If we see table 2 the corresponding residual error E_m given by this approach decreases,however slowly as the order of approximation increases. This kind of behavior of one-step OHAM solution is anticipated and shows the limitation of one-step method as mentioned by Niu and Wang [37]. Although, when the small values of involved physical parameters are taken i.e. $Re = 1$, the one step optimal HAM efficiently calculates the accurate results. Table 3 illustrates the residual error E_m corresponding to the small Reynolds number $(Re = 1)$ and the CPU time in seconds. It is perceived form here that the onestep optimal homotopy analysis method minimizes the square residual error more considerably and much faster as compared to the other optimal approaches. It takes only 18.127 seconds to calculate the 20th order solution of one step optimal HAM approach with the square residual error 1.26406×10^{-27} which is much less as compared with other optimal approaches (see table 3). The corresponding value of $f''(0)$ is given in table 4 and it is noted that after 4th order of approximation, there are no corrections up to 6 decimal places.

Table1: Comparison of $[m,m]$ homotopy padé approximations of $F''(0)$ given by different approaches when $Re = 10, A = 1$ and $Kn_1 = Kn_2 = 1.0$ are kept fixed.

$[m,m]$	One step optimal HAM [37]	1 parameter optimal HAM $c_0 = -1.082301$ $c_1 = c_2 = 0$	2 parameters optimal HAM $c_0 = -1.385313$ $c_1 = c_2 = 0.218662$	3 parameters optimal HAM $c_0 = -1.509902 c_1 = 0.201629$ $c_2 = 0.337949$
[2,2]	−0.398153	−0.410174	−0.410173	−0.409065
[4,4]	−0.417313	−0.409015	−0.409010	−0.409234
[6,6]	−0.413443	−0.409209	−0.409209	−0.409195
[8,8]	−0.410797	−0.409196	−0.409196	−0.409195
[12,12]	−0.410937	−0.409195	−0.409195	−0.409195
[15,15]	−0.409820	−0.409195	−0.409195	−0.409195
[20,20]	−0.409833	−0.409195	−0.409195	−0.409195

Table2: Comparison of the square residual error E_m given by different approaches when $Re = 10, A = 1$ and $Kn_1 = Kn_2 = 1.0$ are kept fixed.

m	One step optimal HAM [37]	1 parameter optimal HAM $c_0 = -1.082301$ $c_1 = c_2 = 0$	2 parameters optimal HAM $c_0 = -1.385313 c_1 = c_2 = 0.218662$	3 parameters optimal HAM $c_0 = -1.509902 c_1 = 0.201629$ $c_2 = 0.337949$
2	9.62619×10^{-1}	8.83605×10^{-1}	8.83538×10^{-1}	6.05501×10^{-1}
4	6.27476×10^{-1}	2.00887×10^{-1}	2.00888×10^{-1}	1.27683×10^{-1}
6	4.78316×10^{-1}	1.05172×10^{-1}	1.05160×10^{-1}	2.13757×10^{-2}
8	3.90369×10^{-1}	3.32121×10^{-2}	3.32137×10^{-2}	3.12835×10^{-3}
12	2.87978×10^{-1}	6.97657×10^{-3}	6.97703×10^{-3}	1.67357×10^{-4}
15	2.41023×10^{-1}	2.70392×10^{-3}	2.70278×10^{-3}	1.99648×10^{-5}
20	1.89059×10^{-1}	4.25642×10^{-4}	4.25642×10^{-4}	3.38389×10^{-7}
25	1.54708×10^{-1}	9.58734×10^{-5}	9.59336×10^{-5}	1.77966×10^{-8}
30	1.30121×10^{-1}	2.27126×10^{-5}	2.27179×10^{-5}	7.36916×10^{-10}

It is interesting to note here that the values of $f''(0)$ given by three parameters optimal approach converge at 2nd order but it is worth mentioning here that the accuracy given by one step optimal approach in fewer time is greatly considerable,though, at same order the accuracy and CPU time required to calculate the solution by one step optimal approach is more appealing as compared to three parameter optimal approach. The time consumed by three parameter approach increases exponentially as the order of approximation increases and it requires 23113.28 seconds to calculate the solution at 20th order of approximation with error 4.81903×10^{-14}.

Table 3: Comparison of E_m and CPU time (seconds) given by different approaches of optimal HAM when $Re = 1.0 A = 1.0$and $Kn_1 = Kn_2 = 1.0$.

m	One step optimal HAM [37]		1 parameter optimal HAM $c_1 = c_2 = 0$		2 parameters optimal HAM $c_1 = c_2 \neq 0$		3 parameters optimal HAM $c_0 \neq c_1 \neq c_2$	
	E_m	CPU time (s)	E_m	CPU time (s)	E_m	CPU time (s)	E_m	CPU time (s)
2	2.77328×10^{-4}	0.094	2.77712×10^{-4}	0.015	2.77712×10^{-4}	0.094	2.49596×10^{-4}	0.094
4	5.35422×10^{-7}	0.312	3.23786×10^{-7}	0.219	3.23786×10^{-7}	0.203	1.84648×10^{-7}	1.138
6	1.39737×10^{-9}	0.780	9.21178×10^{-10}	0.593	9.21178×10^{-10}	3.167	1.77663×10^{-10}	5.101
8	3.50469×10^{-12}	1.388	1.35472×10^{-12}	1.341	1.35484×10^{-12}	9.282	1.54857×10^{-11}	17.987
12	2.51920×10^{-17}	4.212	1.97977×10^{-14}	4.602	8.79793×10^{14}	44.663	1.01558×10^{-12}	223.081
15	3.45111×10^{-21}	8.377	7.63266×10^{-14}	9.547	7.05990×10^{-14}	168.512	4.47737×10^{-13}	1454.16
20	1.26406×10^{-27}	18.127	4.96130×10^{-13}	30.404	3.30552×10^{-12}	950.746	4.81903×10^{-14}	23113.28

Table 4: Comparison of $F''(0)$ given by different approaches when $Re = 1.0 A = 1.0$ and $Kn_1 = Kn_2 = 1.0$ are kept fixed.

m	One step optimal HAM [37]	1 parameter optimal HAM $c_1 = c_2 = 0$	2 parameters optimal HAM $c_1 = c_2 \neq 0$	3 parameters optimal HAM $c_0 \neq c_1 \neq c_2$
2	−0.536056	−0.536052	−0.536052	−0.536057
4	−0.536057	−0.536057	−0.536057	−0.536057
6	−0.536057	−0.536057	−0.536057	−0.536057
8	−0.536057	−0.536057	−0.536057	−0.536057
12	−0.536057	−0.536057	−0.536057	−0.536057
15	−0.536057	−0.536057	−0.536057	−0.536057
20	−0.536057	−0.536057	−0.536057	−0.536057

From tables3 and 4 it is examined that one step optimal approach given by Niu and Wang [37] is computationally more economical, simple and efficient for the case of small Reynolds number Re as compared to other optimal approaches but for some moderate values of Re it losses the accuracy to some extent. In table 5 our current analytic solution is compared with the numerical shooting method and a good agreement is observed between both the techniques

Table 5: Skin friction $-F''(0)$ for the various values of Re,Kn_1, $Kn_2$and A at 20th order of approximation.

Kn_1	Kn_2	Re	A	Current solution by optimal HAM $F''(0)$	Numerical results by Shooting method $F''(0)$
0.0	0.6	2.0	1.0	-0.101915	−0.101915
0.5				-0.053502	−0.053502
1.0				-0.036282	−0.036282
2.0				-0.022075	−0.022075
0.1	0.0		1.0	-4.245316	−4.245316
	0.5			2.178179	2.178179
	1.0			-1.551990	−1.551990
	2.0			-2.072128	−2.072128
0.1	0.6	1.0	1.0	-0.445370	−0.445370
		2.0		-0.086287	−0.086287
		3.0		0.456999	0.456999
		5.0		2.829755	2.829749
0.1	0.6	2.0	0.0	-1.919289	−1.919289
			0.5	-1.106496	−1.106496
			1.0	-0.086287	−0.086287
			2.0	3.184078	3.184078

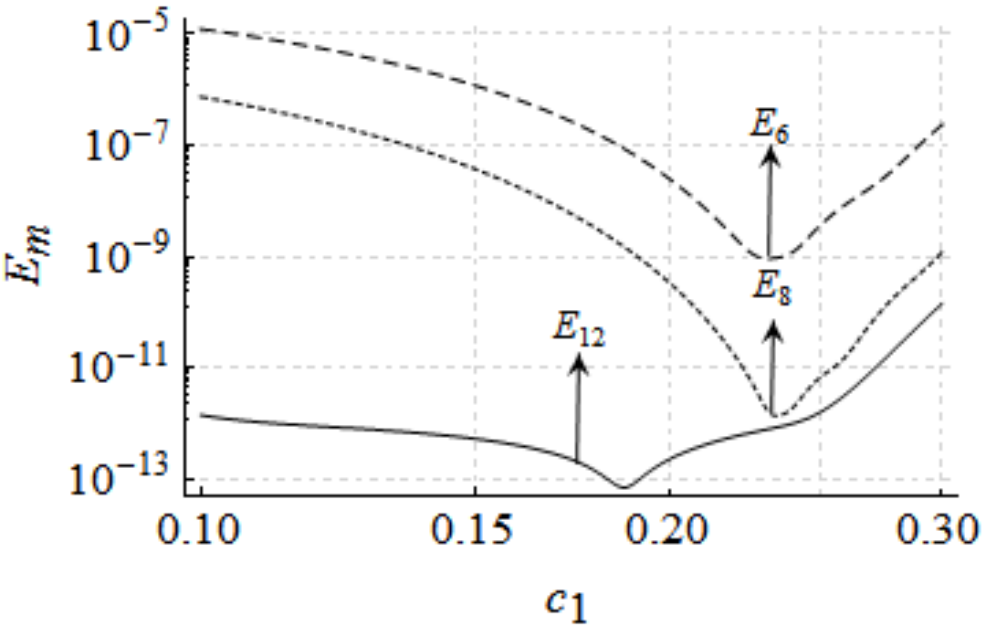

Figure 1: Averaged square residual error E_m versus $c_1$forthe case of two parameter optimal HAM and c_0 is kept fixed at -1.349054, -1.359024 and -1.238944 for 6th, 8th and 12th order of approximation respectively.

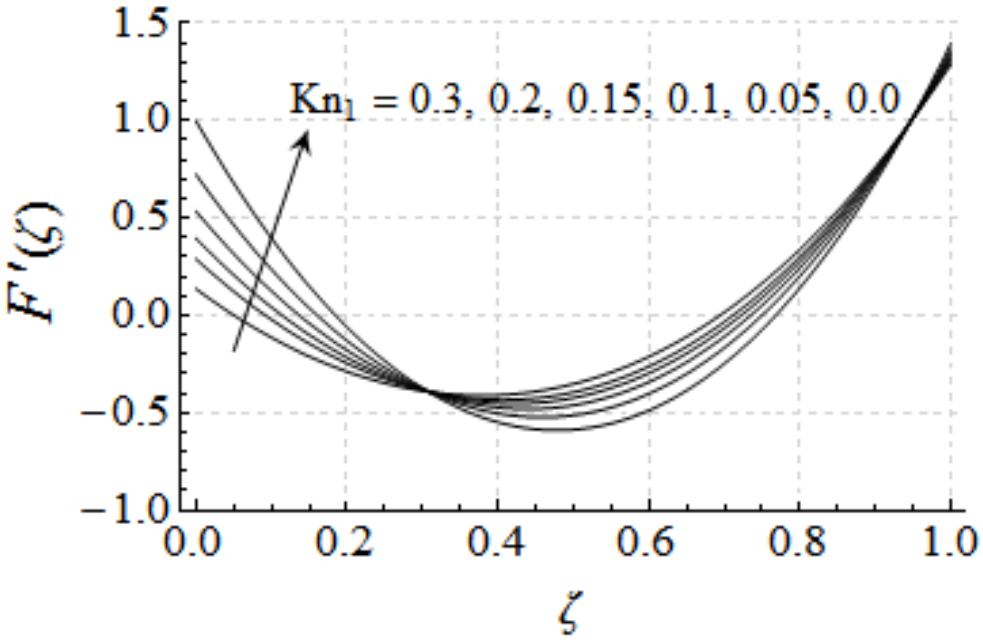

Figure 2: Effects of slip parameter Kn_1on radial velocity when $Re = 2.0$, $A = 1.0$ and $Kn_2 = 0.6$ are held fixed.

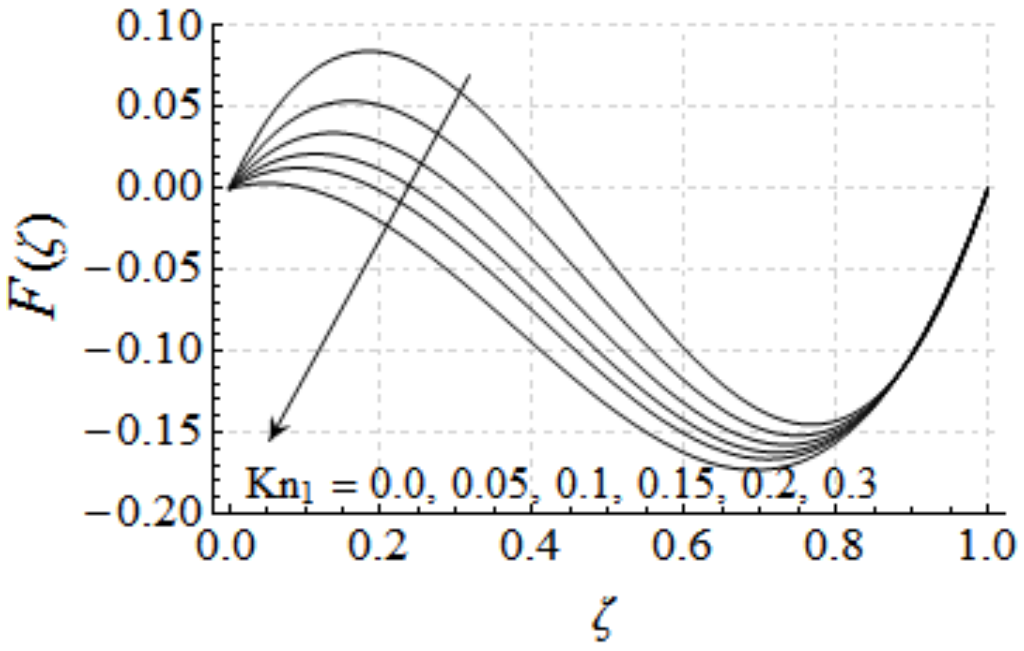

Figure 3: Effects of slip parameter Kn_1on axial velocity when $Re = 2.0$, $A = 1.0$ and $Kn_2 = 0.6$ are held fixed.

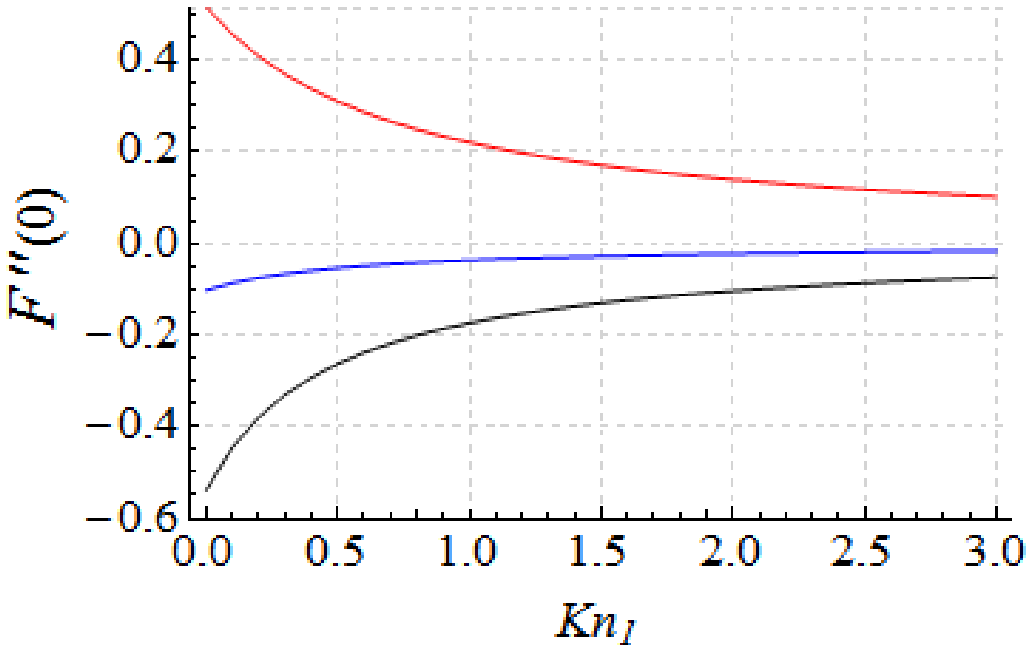

Figure 4: Effects of Re and Kn_1on shear stress at lower disk, Black line $Re = 1$, Blue line $Re = 2$ and Red line $Re = 3$, when $A = 1$ and $Kn_2 = 0.6$ are held fixed.

.

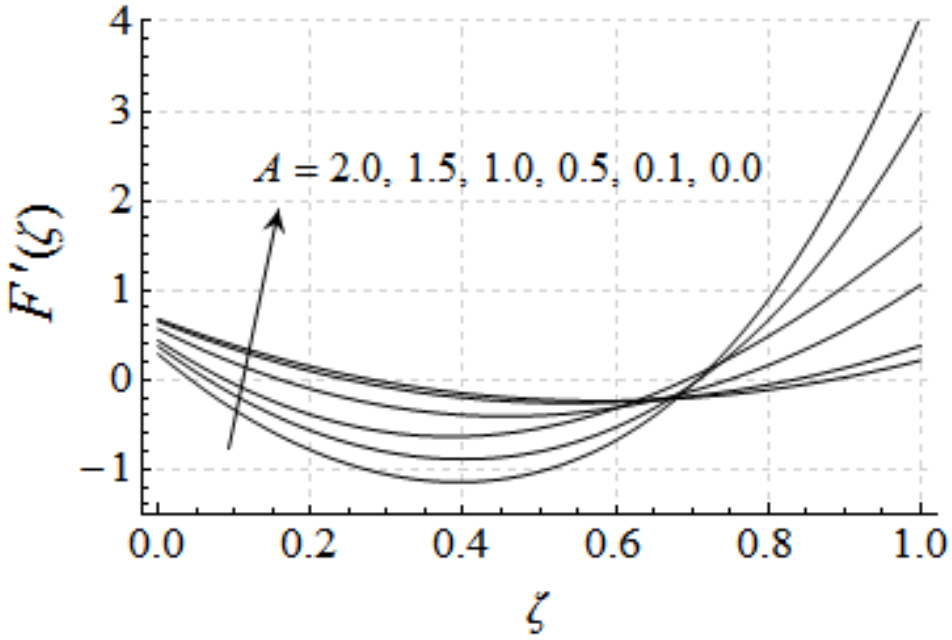

Figure 5: Effects of parameter Aon radial velocity when $Re = 2.0$, $Kn_1 = 0.1$ and $Kn_2 = 0.6$ are held fixed.

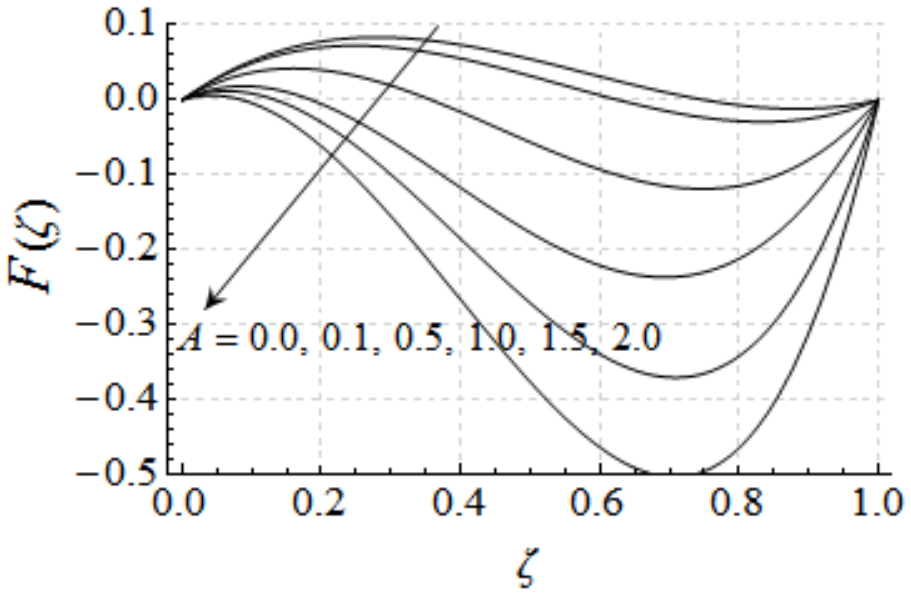

Figure 6: Effects of parameter Aon axial velocity when $Re = 2.0$, $Kn_1 = 0.1$ and $Kn_2 = 0.6$ are held fixed.

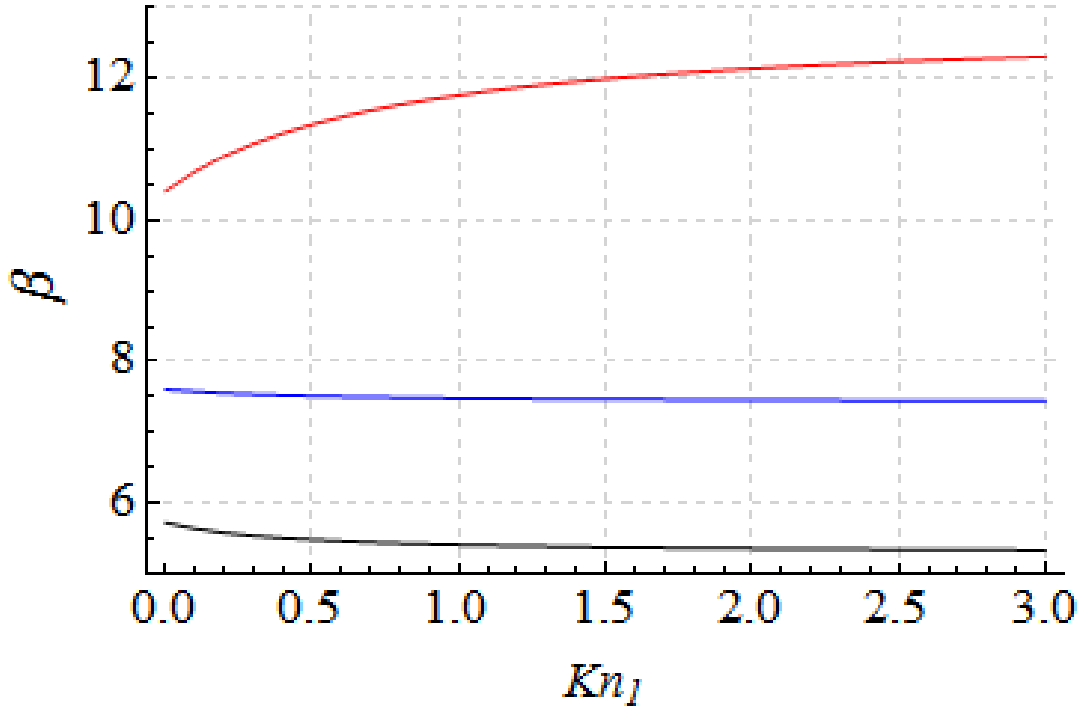

Figure 7: Effects of Re and Kn_1on pressure parameter β, Black line for $Re = 1$, Blue line $Re = 2$ and Red line for $Re = 3$, when $A = 1$ and $Kn_2 = 0.6$ are held fixed.

5. RESULTS AND DISCUSSION

In this section the influences of various physical parameters on the velocity profile and skin friction are illustrated through graphs and tables. The effects of the Knudsen number Kn_1 on the radial and axial velocity profiles are depicted in figures 2 and 3, respectively. From figure 2it is observed that the radial velocity of fluid close to the surfaces of both disks decreases as Kn_1 increases and two points of inflectionoccurin the main flow region at $\zeta = 0.3$ and $\zeta = 0.9$. Thisconduct of the velocity illustrates that as the fluid becomes more rarefied, the velocity at the surfaces of boththe disks reduces. This is because of the reason that the momentum transport in radial direction decreases due to augmentation of slip. In figure 3 the axial velocity is plotted as a function of slip parameter Kn_1 against ζ. From the figure it is observed that the effects of Kn_1 confines near to the surface of lower disk. As Kn_1 increases the axial velocity decreases near the surface of lower disk and no variation occurs in the vicinityof upper disk however, the behavior of the velocity shows that fluid particles flow in upward direction as Kn_1 increases. Figure 4 shows that as the slip parameter Kn_1 increases the skin friction $F''(0)$ decreases drastically and asymptotically approaches to zero.However, it is noticed that for $Re = 1$ and 2 the values of skin friction are negative and beyond these values ($Re = 3$) it takes positive values. Figure 5 shows that as parameter A increases the radial velocity at lower disk reduces and reverse radial flow occurs near the lower disk, nevertheless, it increases near the surface of upper disk. This is mainly due to the reason that as A increases the upper stretching rate becomes dominant over the lower stretching rate and therefore it pushes more fluid particle in radial direction.The graph of axial velocity for various values of A is plotted in figure 6 and it is noticed that the magnitude of axial velocity increases as A increases. It is visible that axial velocity takes negative values and its maximum values occur more significantly in the upper half region. This is due to the fluid particle near upper disk evacuating in radial direction due to great stretching rate, therefore, the particle coming in upward direction are more momentous. Figure 7 illustrates two types of behavior of pressure parameter β; firstly, it decays as Kn_1 increases for small Reynolds number Re and secondly, for large Reynolds number it augments as Kn_1 increases. Although, it is an increasing function of the Reynolds number Re. The numerical values of skin friction coefficient at lower disk are illustrated in table 5 for different values of parameters Kn_1, Kn_2, Re and A. The table shows that the shear stress at lower disk decreases byincreasing Kn_1. It is noted that the skin friction change its values from negative to positive when $Kn_2 = 0.5$ and afterwards it again takes negative values and the magnitude of $F''(0)$ increases by increasing Kn_2. It is observed that for small Reynolds number the skin friction takes negative values and by increasing the Reynolds number it changes the sign and the magnitude augments. The values of skin friction show that as A increases it diminishes toward zero and for large A it augments with positive values which indicate the reverse radial flow.

6. CONCLUSION

In this study the effects of partial slip condition on steady laminar flow between two stretchable disk have been investigated. The objective of the study is twofold; first to explore the physics of flow and second to identify the best analytic technique towards the solution of nonlinear governing equations arising in the study of fluid flows. Apparently, the physics of the flow can be studied if one has the solution of the problem in hand. Therefore, it is reasonable to embark on the solution part first.

In this study we used optimal homotopy analysis method through different approaches to solve the governing nonlinear equation. We used the one step optimal HAM, the one parameter, two parameters and three parameters optimal HAM approaches. Since in the study of nonlinear differential equations it is impossible to suggest a single solution method to be useful anyways, the same happened with the present study. In our analysis it is observed that for the case of large Reynolds number the one step optimal HAM converges to the exact solution very slowly reflecting that the approximation will reach the exact solution after hundreds of iterations which might be impossible to reach for an ordinary PC. Whereas on the other hand, for the same case considered, it is observed that the three parameters optimal HAM converges faster and accurately than the rest three. But the CPU time of three parameters optimal HAM is very large which is not economical from the computational point of view. On the other hand, if we consider the case of the small Reynolds number,the one step optimal HAM gives very accurate results in very short time as compared to the three parameters optimal HAM. In this case one step optimal HAM takes 18.127 sec and three parameters method takes 23113.28 sec which is very large. From above arguments we are of the opinion that all the proposed homotopy techniques are useful within the range of their implications. Therefore, while dealing with nonlinear problems one should check if the problem is less complicated, then the traditional HAM or one step optimal HAM are useful, but if the problem is more complicated, then one should move towards the one parameter, two parameters or three parameters optimal HAM. One thing which is of great importance is that the computations required for two or three parameters optimal HAM is very much high.

On physical side, it is observed that the involvement of the Knudsen number Kn_1 in the velocity expression affects the velocity at the surfaces of disks. The effect of slip parameter Kn_1 is to reduce the velocity at the surfaces of disks. Also an increase in the Knudsen number Kn_1 causes to decrease the skin fiction at the lower disk. It is concluded that the radial velocity increases near the upper disk as A increases and reverse flow occurs near the lower disk at sufficiently large A. Due to an increment in the Reynolds number the skin friction at lower disk increases. The pressure parameter is a decreasing function of Kn_1 for small Re and an increasing function of Kn_1 for large Re.

REFERENCES

1. I. Vleggaar, Laminar boundary-layer behavior on continuous accelerating surfaces, Chem. Engng. Sci., 32 (1977) 1517-1525.
2. B.C. Sakiadis, Boundary-layer behavior on continuous solid surfaces: I. Boundary-layer equations for two-dimensional and axisymmetric flow,AIChE J., 7 (1961) 26-28.
3. L.J. Crane, Flow past a stretching plate, Z. Angew. Math. Phys., 21, (1970) 645.
4. C.Y. Wang,The three-dimensional flow due to a stretching flat surface, Phys. Fluids, 27 (1984) 1915.
5. H.I. Andersson, MHD flow of a viscoelastic fluid past a stretching surface, Acta Mech., 95 (1992) 227-230.
6. W.C. Troy, E.A. Overman II, G.B. Eremont-Rout, J.P. Keener, Uniqueness of flow of second order fluid past a stretching sheet, Q. Appl. Math., 44 (1987) 753-755.
7. P. Carragher, L.J. Crane, Heat transfer on a continuous stretching sheet, ZAMM, 62 (1982) 564-565.

8. L.J. Grubka, K.M. Bobba, Heat transfer characteristics of a continuous stretching surface with variable temperature, ASME J. Heat Transfer, 107 (1985) 248-250.
9. M. Kumari, H.S. Takhar, G. Nath, MHD flow and heat transfer over a stretching surface with prescribed wall temperature or heat flux, WärmeStoffübertr, 25 (1990) 331-336.
10. E.M.A. Elbashbeshy, Heat transfer over a stretching surface with variable surface heat flux, J. Phys. D: Appl. Phys., 31 (1998) 1951-1954.
11. A. Ali, A. Mehmood, Homotopy analysis of unsteady boundary layer flow adjacent to permeable stretching surface in a porous medium, Commun. Non Linear Sci. Numer. Simul., 13 (2008) 340-349.
12. A. Mehmood, A. Ali, Analytic solution of generalized three-dimensional flow and heat transfer over a stretching plane wall, Int. Commun. Heat Mass Transfer, 33 (2006) 1243-1252.
13. C.Y. Wang, Fluid flow due to a stretching cylinder, Phys. Fluids 31 (3) (1988) 466-468.
14. P.D. Ariel, Axisymmetric flow of a second grade fluid past a stretching sheet, Int. J. Eng. Sci. 39 (2001) 529-553.
15. T. Fang, Flow over a stretchable disk, Phy. Fluids, 19 (2007) 128105.
16. M.B. Zaturska, W.H.H. Banks, New solutions for flow in a channel with porous walls and/or non-rigid walls, Fluid Dynamics Research 33 (1-2) (2003) 57-71.
17. T. Fang, J. Zhang, Flow between two stretchable disks-An exact solution of the Navier-Stokes equations. Int. Commun. Heat Mass Transfer 35 (2008) 892-895.
18. A. Robert, V. Gorder, E. Sweet, K. Vajravelu, Analytical solutions of a coupled nonlinear system arising in a flow between stretching disks, Appl. Math. Comput. 216 (2010) 1513-1523.
19. Shijun Liao, An optimal homotopy-analysis approach for strongly nonlinear differential equations, Commun. Nonlinear Sci. Numer. Simul.,15 (2010) 2003-2016.
20. S.J. Liao, The proposed homotopy analysis technique for the solution of nonlinear problems, PhD thesis, Shanghai Jiao Tong University; 1994.
21. S.J. Liao, A kind of approximate solution technique which does not depend upon small parameters (II): an application in fluid mechanics, Int. J. Non-Linear Mech., 32 (1997) 815-22.
22. S.J. Liao, Notes on homotopy analysis method: some definitions and theorems, Commun. Nonlinear Sci. Numer. Simul., 14 (2009) 983-97.
23. Z. Ziabaksh, G. Domairy, Solution of the laminar viscous flow in a semi-porous channel in the presence of uniform magnetic field by using the homotopy analysis method, Commun. Nonlinear Sci. Numer. Simmul.,doi: 10.1016/j.cnsns.2007.12.011.
24. F.M. Allan, M.I. Syam, On analytic solution of the non-homogeneous Blasius Problem, J. Comp. Appl. Math.,182 (2005) 355-365.
25. M. Khan, S. Munawar and S. Abbasbandy, Steady flow and heat transfer of a Sisko fluid in annular pipe, Int. J. Heat Mass Transf.,53 (2010) 1290–1297.
26. A. Mehmood, A. Ali, T. Shah, Unsteady boundary-layer viscous flow due to an impulsively started porous plate, Canadian J. Phys.,86 (2008) 1079-1082.
27. A. Mehmood, A. Ali, H.S. Takhar, T. Shah, Corrigendum to: "Unsteady three dimensional MHD boundary layer flow due to the impulsive motion of a stretching surface (Acta Mech. 146, 59-71 (2001))",ActaMechanica, 199 (2008) 241-249.

28. H. Xu, S.J. Liao, Series solutions of unsteady Magnetohydrodynamic flows of non-Newtonian fluids caused by an impulsively stretching plate, J Non-Newtonian Fluid Mech., 129 (2005) 46-55.
29. S.J. Liao, An analytic solution of unsteady boundary layer flows caused by an impulsively stretching plate, Commun. Non-Linear Sci. Numer. Simul., 11 (2006) 326-39.
30. A. Mehmood, A. Ali, Unsteady boundary layer flow due to an impulsively started moving plate, Proc. IMechE. Part F: J. Aerospace Eng.,221 (2007) 385-390.
31. A. Mehmood, S. Munawar and A. Ali, Letter to the editor Comment on: "Homotopy analysis method for solving the MHD flow over a non-linear stretching sheet (Commun. Nonlinear Sci. Numer. Simul. 14 (2009) 2653–2663)", Commun. Non-linear Sci. Numer. Simul.,15 (2010) 4233–4240.
32. S. Abbasbandy, Homotopy analysis method for heat radiation equations, Int.Commun. Heat Mass Transfer, 34 (2007) 380–387.
33. S. Abbasbandy, Z.F. Samadian, Soliton solutions for the fifth-order KdVequation with homotopy analysis method, Nonlinear Dyn., 51 (2008) 83–87.
34. S.J. Liao, An explicit, totally analytic approximation of Blasius viscous flow problems, Int. J. Non-Linear Mech., 34(40) (1999) 759-78.
35. V. Marinca, N. Herisanu, L. Nemes, Optimal homotopy asymptotic method with application to thin film flow, Cent. Eur. J. Phys., 6(3) (2008) 648-653.
36. K. Yabushita, M. Yamashita, K. Tsuboi, An analytic solution of projectile motion with the quadratic resistance law using the homotopy analysis method, J. Phys. A: Math. Theor, 40 (2007) 8403-8416.
37. Z. Niu, C. Wang, A one-step optimal homotopy analysis method for nonlinear differential equations, Commun. Nonlinear. Sci. Numer. Simul., 15 (2010) 2026-2036.